A Novel FMCW Radar-Based Scheme for Indoor Localization and Trajectory Tracking

Xiangyu Shen
College of Physics and Information Engineering
Fuzhou University
Fuzhou, Fujian, China
e-mail: xyshen1998@163.com

Haifeng Zheng
College of Physics and Information Engineering
Fuzhou University
Fuzhou, Fujian, China
e-mail: zhenghf@fzu.edu.cn

Xinxin Feng
College of Physics and Information Engineering
Fuzhou University
Fuzhou, Fujian, China
e-mail: fxx1116@fzu.edu.cn

2020 IEEE 6th International Conference on Computer and Communications (ICCC) | 978-1-7281-8635-1/20/$31.00 ©2020 IEEE | DOI: 10.1109/ICCC51575.2020.9345047

***Abstract*—In recent years, with the rapid development of the Internet of Things (IoT) related technologies, the location-based service (LBS) has attracted increasing attention. Frequency modulated continuous wave (FMCW) is a promising technique for indoor localization due to its low deployment costs and strong anti-interference ability. In this paper, we develop a novel FMCW radar-based positioning scheme for indoor localization and target trajectory detection. In particular, we propose an OSCA-CFAR algorithm with star-shaped reference sliding window to improve the accuracy of indoor positioning. Furthermore, the extended Kalman filter is introduced into the scheme to solve the nonlinear problem of motion trajectory tracking. Finally, we carry out extensive experiments with a real testing platform. Experimental results demonstrate that the proposed scheme is able to achieve better performance compared with the existing schemes.**

Keywords- Indoor localization, FMCW radar, trajectory tracking, CFAR, extended kalman filter

I. INTRODUCTION

With the rapid development of IoT related technologies, the Location-Based Service (LBS) industry has witnessed rapid growth. However, due to the building shielding and other factors, the highly mature satellite positioning technology in the outdoor environment cannot provide high-precision positioning information in the indoor environment [1]. At present, indoor positioning technology is widely used in indoor navigation, fire site rescue, smart home, and many other fields [2].

In order to improve the positioning accuracy of the indoor environment, many indoor positioning technologies have appeared in recent years, such as Wi-Fi positioning, Radio Frequency Identification (RFID), and Bluetooth and ultrawideband (UWB) radio positioning. Besides the above positioning techniques, frequency modulated continuous wave (FMCW) has become a promising positioning technique due to its many advantages in anti-jamming and positioning accuracy [3].

In recent years, many efforts have been made to improve FMCW radar-based positioning performance. For example, Katabi et al. [4] [5] developed WiTrack, an indoor positioning system that uses human radio reflection for 3D tracking. By receiving signals reflected from a moving human body and conducting 3D modeling to determine the human body's position, the accuracy can reach 10-21cm. Jia et al. [6] proposed an indoor stationary human body detection algorithm based on FMCW radar, which uses life signal detection and ellipse cross-location to locate human. Wang et al. [7] proposed a hybrid radar scheme that combines interferometric radar and FMCW radar for indoor positioning. Xiong et al. [8] also proposed a linear FMCW radar-based system with an improved constant-false-alarm rate (CFAR) algorithm for indoor positioning and moving target trajectory tracking.

However, the current works still face some challenges. On one hand, due to the numerous objects, walls, etc, there are various noises caused by multi-path interference in the indoor environment, which are mixed in the echo signal received by the receiving antennas reducing the positioning accuracy of FMCW radar. On the other hand, the current works on FMCW radar-based indoor positioning have not efficiently solved the problem of the moving targets' trajectory tracking. Since a target's motion is usually nonlinear, if it does not consider this characteristic in the trajectory estimation algorithm, it is easy to bring cumulative errors and cannot achieve high-precision performance for trajectory tracking.

In this paper, we develop an FMCW radar-based positioning scheme for indoor localization and target trajectory detection to tackle the above issues. The main contributions of this paper are summarized as follows:

- To eliminate the influence of background noise on positioning accuracy, we propose the OSCA-CFAR algorithm with star-shaped reference sliding window.

The algorithm can solve the problem of positioning accuracy degradation caused by background noise in an indoor environment.

- To cope with the nonlinear characteristics of human motion trajectory, we introduce the extended Kalman filter (EKF) into the scheme to improve the performance of target trajectory tracking.
- We carry out extensive experiments to evaluate the performance of the proposed scheme. The experimental results show that the proposed scheme can improve the accuracy of indoor localization and trajectory tracking for moving targets.

The rest of the paper is organized as follows: the basic theory of FMCW positioning is introduced in Section II. Then FMCW radar-based positioning algorithms are proposed in Section III. In Section IV, the experimental results are provided. The conclusion is drawn in Section V.

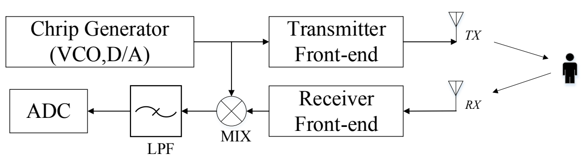

Figure 1: The block diagram of the FMCW radar.

II. THE PRINCIPLE OF FMCW RADAR POSITIONING

Fig. 1 shows a paradigm of an FMCW positioning system. A voltage-controlled oscillator (VCO) is used to generate FM signals with regular frequency changes over time. The transmitting antenna sends part of the signals, and the other part is coupled with the echo signals reflected by the target. A low-pass filter filters the beat signal. The beat signal is processed by an ADC to convert it into the range, angle for positioning [9].

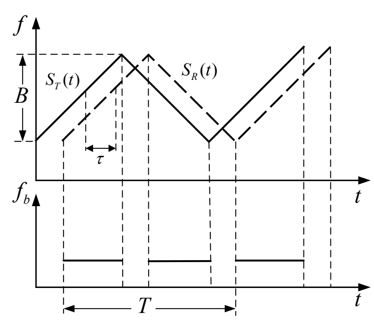

Figure 2. FMCW radar waveform.

A. Range Measurement

Fig. 2 shows the frequency of FMCW radar, which changes linearly with time. The solid line presents the transmitting signal frequency, the dashed line denotes the receiving signal frequency. The transmit signal frequency can be written as:

$$f_T(t) = f_0 + \frac{df}{dt}t = f_0 + \frac{2B}{T}t, \tag{1}$$

and the received signal frequency can be expressed as:

$$f_R(t) = f_0 + \frac{df}{dt}(t-\tau) = f_0 + \frac{2B}{T}(t-\tau), \tag{2}$$

where $\tau = 2R/c$ is the propagation delay. By applying the Fourier transform to the mixed signal passing through the low-pass filter, we can get the beat signal frequency f_b, which contains the information of the target:

$$f_b = \frac{2B}{T}\tau \tag{3}$$

The range of the target is calculated from (4) in which c is the speed of light, and B is the transmitting signal bandwidth:

$$R = \frac{c\tau}{2} = \frac{cT}{2B}f_b. \tag{4}$$

B. Angle Measurement

Besides, since the difference of signal propagation distance will cause the change of phase, we can calculate the phase difference $\Delta\varphi$:

$$\Delta\varphi = \omega\frac{\Delta d}{c} = \frac{2\pi\Delta d}{\lambda} = \frac{2\pi l\sin(\theta)}{\lambda} \tag{5}$$

where λ is the wavelength of the FMCW radar signal. And as shown in Fig. 3, l is the distance between two adjacent receiving antennas, and $\Delta d = l\sin(\theta)$ is the propagation distance between adjacent antennas. Thus, the incidence Angle of the target θ can be calculated by:

$$\theta = \sin^{-1}\left(\frac{\lambda\Delta\varphi}{2\pi l}\right). \tag{6}$$

C. Positioning Principle

With the range and incident angle of the target, we can calculate the target's position according to the geometric relationship. Fig. 4 shows the positioning principle based on the range and the angle of incidence.

Assuming that the coordinate of the target is (x, y), the position of the target can be written as:

$$\begin{cases} x = R\sin(\theta) \\ y = \sqrt{R^2 - x^2} \end{cases}, \tag{7}$$

where R is the range of target, θ is the angle of incidence of echo signal, Thus the relative position information of the target can be obtained.

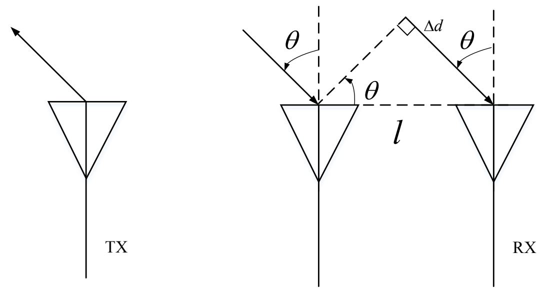

Figure 3. Incidence Angle estimation.

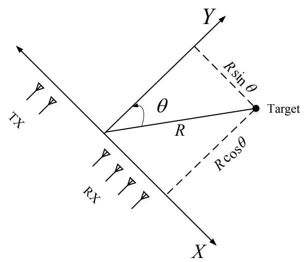

Figure 4. FMCW radar localization system.

III. The Proposed FMCW Radar Based Positioning

According to the principle of FMCW radar positioning, we develop an indoor positioning scheme for stationary target positioning and moving target tracking. The data processing procedure for indoor positioning is shown in Fig. 5. Since noise and interference always exist in the measurement, the positioning performance will be affected by them. How to relieve their impact is a key issue for indoor positioning. In this scheme, an improved OSCA-CFAR algorithm and an EKF algorithm are proposed to offset the influence of noise and interference and improve the scheme's positioning accuracy.

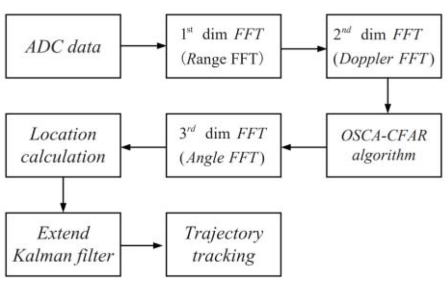

Figure 5. Data processing procedure for indoor positioning.

A. The Improved OSCA-CFAR Algorithm

In this section, we introduce the CFAR algorithm, which can adaptively adjust its sensitivity according to the noise and interference intensity change while keeping the radar false alarm probability constant [10]. The CFAR detector first processes the input noise and determines a threshold, and compares it with the input signal. If the input signal exceeds this threshold, it is judged as a target; otherwise, it is deemed as no target.

As we know, the cells averaging constant false alarm rate (CA-CFAR) algorithm has the disadvantages of multi-target masking and poor false alarm performance of clutter edge region. Besides, the order statistics constant false alarm rate (OS-CFAR) algorithm requires high computation complexity, and the false alarm probability of clutter edge region is increased, which degrades the performance of the CFAR algorithm [11]. Therefore, we propose the OSCA-CFAR algorithm, which integrates the above two algorithms to improve the performance.

OSCA-CFAR algorithm increases the number of training units and improves the robustness of the algorithm. Besides, due to the specific ordering of training units in the doppler dimension, the OSCA-CFAR algorithm avoids the problem of the high computational complexity of OS-CFAR algorithm and greatly reduces the computation time[12]. Furthermore, we explore the influence of the reference slide window's shape on the OSCA-CFAR algorithm' performance.

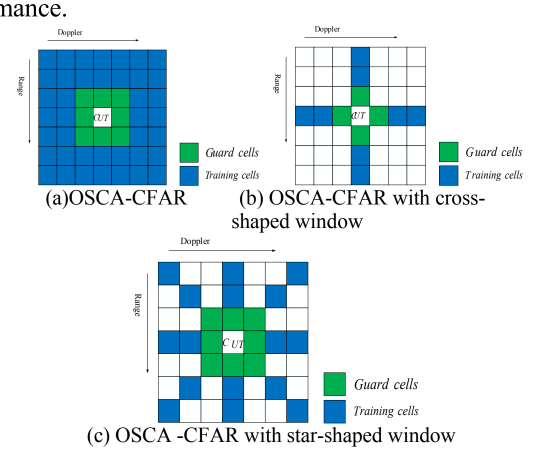

Figure 6. OSCA-CFAR algorithm for three different slide window shapes

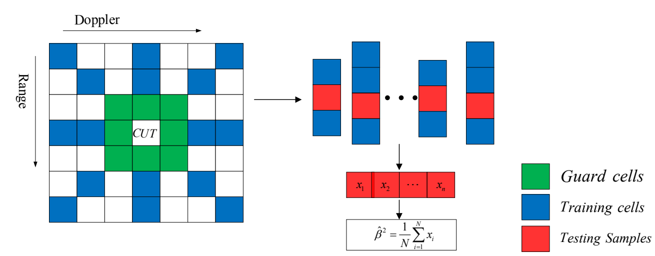

Figure 7. The OSCA-CFAR algorithm with star-shaped sliding.

As shown in Fig. 6(a), the rectangular reference sliding window is used in the original OSCA-CFAR algorithm, which requires high computation resources since it needs a number of training units. In Fig. 6(b), a cross-shaped reference sliding window is utilized to reduce the number of training units. However, it incurs the degraded positioning performance. In this paper, we propose an OSCA-CFAR algorithm with star-shaped sliding by adding training units as shown in Fig. 6(c), which not only reduces the computation complexity compared with the original OSCA-CFAR algorithm but also improves positioning performance.

As shown in Fig. 7, the data processing procedure of OSCA-CFAR algorithm includes the following steps:

- Step I: In the range dimension, a one-dimensional OS-CFAR detector is used for the training unit, and each column selects the k-th largest unit as the samples for testing.

- Step II: The testing samples are collected and use a one-dimensional CA-CFAR detector in the Doppler dimension to improve the accuracy of clutter power level estimation [13].

B. *Extended Kalman Filter for Trajectory Tracking*

In our scheme, we also introduce EKF to combat the trajectory tracking accuracy decline caused by the nonlinear feature of the human motion [14]. The EKF expands the nonlinear state transfer function and observation function in the system with Taylor series, abandons the second-order and higher-order terms, linearizes the system in the first order.

Firstly, we use the state transition and observation functions to describe the system:

$$\theta_k = f\left(\theta_{k-1}\right) + \mathbf{s}_k \tag{8}$$

$$\mathbf{z}_k = h\left(\theta_k\right) + \mathbf{v}_k \tag{9}$$

where θ_k is the true system state, z_k is the observed system state, s_k and v_k are observation noise and model noise, respectively, which obey Gaussian distribution.

Using the Taylor expansion to expand (8) at the last estimated value of $\left\langle \theta_{k-1} \right\rangle$, we can obtain:

$$\theta_k = f\left(\theta_{k-1}\right) + \mathbf{s}_k = f\left(\theta_{k-1}\right) + \mathbf{F}_{k-1}\left(\theta_{k-1} - \left(\theta_{k-1}\right)\right) + \mathbf{s}_k \tag{10}$$

Then we expand the Taylor expansion to (9) in the current round of state prediction value $\theta_k^{'}$:

$$\mathbf{z}_k = h\left(\theta_k\right) + \mathbf{v}_k = h\left(\theta_k^{'}\right) + \mathbf{H}_k\left(\theta_k - \theta_k^{'}\right) + \mathbf{v}_k \tag{11}$$

where F_{k-1} and H_k respectively represent the Jacobian matrix of functions $f(\theta)$ and $h(\theta)$ at $\left\langle \theta_{k-1} \right\rangle$ and θ_k , and z_k is actual observed value.

In the above derivation, only the Taylor expansion of the first derivative is retained, while the derivatives of the second and above are ignored. Based on the above equations, prediction and update steps of EKF can be deduced as follows:

Prediction:

$$\begin{cases} \theta_k = f(\theta_{k-1}) \\ \Sigma_k^{'} = F_{k-1}\Sigma_{k-1}F_{k-1}^{T} + Q \end{cases} \tag{12}$$

Update:

$$\begin{cases} \boldsymbol{S}_k^{'} = \left(\boldsymbol{H}_k\boldsymbol{\Sigma}_k^{'}\boldsymbol{H}_k^{T} + \boldsymbol{R}\right)^{-1} \\ \boldsymbol{K}_k^{'} = \boldsymbol{\Sigma}_k^{'}\boldsymbol{H}_k^{T}\boldsymbol{S}_k^{'} \\ \theta_k = \theta_k^{'} + K_k^{'}\left(\boldsymbol{z}_k - h(\theta_k)\right) \\ \boldsymbol{\Sigma}_k = \left(\boldsymbol{I} - \boldsymbol{K}_k^{'}\boldsymbol{H}_k\right)\boldsymbol{\Sigma}_k^{'} \end{cases} \tag{13}$$

In the prediction stage, the predicted value of the error $\Sigma_k^{'}$ between the estimated value and the real value is also given for adjusting the prediction model, Q is the covariance matrix of the observed noise. In the updated stage, the model updates the observation noise $S_k^{'}$ and the Kalman coefficient $K_k^{'}$ respectively, and R is the covariance matrix of the observed noise. Besides, the feedback mechanism is introduced into the model. The model is modified by the difference between the predicted value and the real observed value to achieve better prediction results.

In the algorithm, we use EKF to process the independent position points which have been processed by the CFAR detector to obtain the estimated trajectory.

IV. EXPERIMENTAL RESULTS

As shown in Fig. 8, we built a testing platform with TI's IWR1642-Boost development board and use DCM100 high-speed data acquisition card to capture the echo data. The frequency range of the FMCW radar wave is 77.18GHz ~ 78.72GHz, and bandwidth is 1.54GHz. Two transmitting antennas and four receiving antennas are set on the radar, which can simulate eight antennas. The range resolution of the radar is about 9.76cm, and the angular resolution is 14.43∘. We import radar echo data into MATLAB to evaluate the performance of the proposed algorithm. Each frame of data contains 256 samples in the range dimension and 64 samples in the doppler dimension. The echo signal contains 250 frames.

Figure 8. FMCW radar used in the experiment.

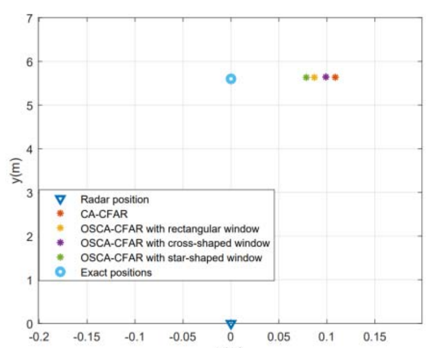

Figure 9. Exact and estimated locations of stationary targets.

A. *Stationary Target Detection*

In the experiment, a stationary target is placed at 5.6m in front of the radar, and different CFAR detectors are used to process the radar echo and obtain the location information of the target. The location results are shown in Fig. 9. We use root mean square error (RMSE) and median absolute error (MAE) to measure the positioning accuracy. Location range error results, and X and Y axis error distributions are shown in Table I.

TABLE I. THE PERFORMANCE OF STATIONARY TARGET POSITIONING

	CA-CFAR	OSCA-CFAR with rectangular window	OSCA-CFAR with cross-shaped window	OSCA-CFAR with star-shaped window
RMSE	0.1066m	0.0850m	0.0989m	0.0628m
MAE	0.1040m	0.0859m	0.0981m	0.0612m
X axis error	0.1087m	0.0909m	0.0989m	0.0875m
Y axis error	0.365m	0.0338m	0.0438m	0.0329m

As can be seen from the results, the OSCA-CFAR algorithm has better performance than CA-CFAR algorithm. Compared with CA-CFAR algorithm, the average positioning accuracy of the OSCA-CFAR with star-shaped reference sliding window algorithm is improved by 41.08%, and MAE is reduced by 41.13%. Furthermore, different sliding windows affect the performance of the CFAR algorithm. The OSCA-CFAR algorithm with a star-shaped reference sliding window improves positioning performance since it increases training units in the diagonal direction compared with the OSCA-CFAR algorithm with a cross-shaped sliding window.

Besides, we also find that the OSCA-CFAR algorithm can improve the positioning accuracy in the X-axis and Y-axis directions, respectively. It can be also observed that the X-axis error is greater than the Y-axis error. This is because the insufficient spacing of the receiving antenna array leads to lower resolution in X-axis than that in Y-axis.

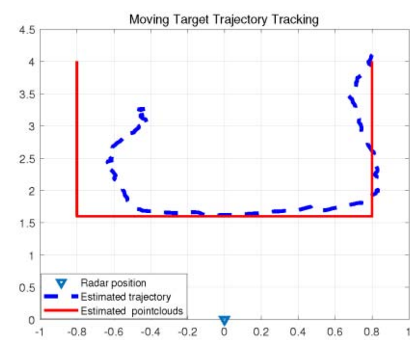

(a) OSCA-CFAR with star-shaped window + KF

(b) OSCA-CFAR with star-shaped window +EKF

Figure 10. Moving target trajectory tracking.

B. *Moving Target Trajectory Tracking*

In the trajectory tracking experiment, a person moves from the top left corner by following a predetermined trajectory. In the experiment, we apply the OSCA-CFAR algorithm with a star-shaped reference slide window to process the radar echo signal and then use EKF to track the target trajectory. The experimental results are shown in Fig. 10, and error statistics results are given in Table. II.

TABLE II. TABLE TYPE STYLES

	KF	EKF	Improvement
RMSE	0.1109m	0.0852m	23.17%
MAE	0.0882m	0.0854m	3.17%

The experimental results show that EKF can track the moving target trajectory more accurately than KF, which improves the average positioning accuracy by 23.17% compared with KF under the same conditions.

V. CONCLUSION

In this paper, we developed an FMCW radar-based positioning scheme for indoor localization and target trajectory detection. We proposed an OSCA-CFAR algorithm with starshaped reference sliding window to improve the accuracy of indoor localization. Furthermore, the EKF is introduced into the algorithm to tackle the nonlinear characteristics of motion trajectory tracking. Experimental results demonstrated the effectiveness of the proposed scheme.

REFERENCES

[1] H. Liu, H. Darabi, P. Banerjee, and J. Liu, "Survey of wireless indoor positioning techniques and systems," IEEE Transactions on Systems, Man, and Cybernetics, Part C (Applications and Reviews), vol. 37, no. 6, pp. 1067–1080, 2007.

[2] G. Oguntala, R. Abd-Alhameed, S. Jones, J. Noras, M. Patwary, and J. Rodriguez, "Indoor location identification technologies for real-time iot-based applications: An inclusive survey," Computer Science Review, vol. 30, pp. 55–79, 2018.

[3] M. S. Mahmud, S. U. Qaisar, and C. Benson, "Weak gps signal detection in the presence of strong signals with varying relative doppler and long integration gain," in 2016 IEEE/ION Position, Location and Navigation Symposium (PLANS), pp. 1015–1020, IEEE, 2016.

[4] F. Adib, Z. Kabelac, D. Katabi, and R. C. Miller, "3d tracking via body radio reflections," in 11th USENIX Symposium on Networked Systems Design and Implementation (NSDI 14), pp. 317–329, 2014.

[5] F. Adib, Z. Kabelac, and D. Katabi, “Multi-person localization via rf body reflections,” in 12th USENIX Symposium on Networked Systems Design and Implementation (NSDI 15), pp. 279–292, 2015.

[6] Y. Jia, L. Kong, X. Yang, and K. Wang, “Through-wall-radar localization for stationary human based on life-sign detection,” in 2013 IEEE Radar Conference (RadarCon13), pp. 1–4, IEEE, 2013.

[7] G. Wang, J.-M. Munoz-Ferreras, C. Gu, C. Li, and R. Gomez-Garcia, “Application of linear-frequency-modulated continuous-wave (lfmcw) radars for tracking of vital signs,” IEEE transactions on microwave theory and techniques, vol. 62, no. 6, pp. 1387–1399, 2014.

[8] R. Xiong, X. Feng, H. Zheng, and Z. D. Chen, “Linear fmcw radar system for accurate indoor localization and trajectory detection,” in 2020 International Conference on Computing, Networking and Communications (ICNC), pp. 741–745, IEEE, 2020.

[9] J. Hao, T. Huang, Z. D. Chen, H. Zhao, and J. Li, “A gnu radio based fmcw radar with a simple frequency correction technique for accurate indoor localization applications,” in 2018 IEEE MTT-S International Wireless Symposium (IWS), pp. 1–4, IEEE, 2018.

[10] F. Colone, D. W. O’Hagan, P. Lombardo, and C. Baker, “A multistage processing algorithm for disturbance removal and target detection in passive bistatic radar,” IEEE Transactions on Aerospace and Electronic Systems, vol. 45, 2009.

[11] X. W. Meng, “Performance analysis of os-cfar with binary integration for weibull background,” IEEE Transactions on Aerospace and Electronic Systems, vol. 49, no. 2, pp. 1357–1366, 2013.

[12] M. Kronauge and H. Rohling, “Fast two-dimensional cfar procedure,” IEEE Transactions on Aerospace and Electronic Systems, vol. 49, no. 3, pp. 1817–1823, 2013.

[13] A. Maali, A. Mesloub, M. Djeddou, H. Mimoun, G. Baudoin, and A. Ouldali, “Adaptive ca-cfar threshold for non-coherent ir-uwb energy detector receivers,” IEEE Communications Letters, vol. 13, no. 12, pp. 959–961, 2009.

[14] M. S. Arulampalam, S. Maskell, N. Gordon, and T. Clapp, “A tutorial on particle filters for online nonlinear/non-gaussian bayesian tracking,” IEEE Transactions on signal processing, vol. 50, no. 2, pp. 174–188, 2002